

Energy Dissipation and Landau Damping in Two- and Three-Dimensional Plasma Turbulence

Tak Chu Li¹, Gregory G. Howes¹, Kristopher G. Klein² and Jason M. TenBarge³

¹*Department of Physics and Astronomy, University of Iowa, Iowa City, Iowa 52242, USA*

²*Space Science Center, University of New Hampshire, Durham, New Hampshire 03824, USA*

³*IREAP, University of Maryland, College Park, Maryland 20742, USA*

ABSTRACT

Plasma turbulence is ubiquitous in space and astrophysical plasmas, playing an important role in plasma energization, but the physical mechanisms leading to dissipation of the turbulent energy remain to be definitively identified. Kinetic simulations in two dimensions (2D) have been extensively used to study the dissipation process. How the limitation to 2D affects energy dissipation remains unclear. This work provides a model of comparison between two- and three-dimensional (3D) plasma turbulence using gyrokinetic simulations; it also explores the dynamics of distribution functions during the dissipation process. It is found that both 2D and 3D nonlinear gyrokinetic simulations of a low-beta plasma generate electron velocity-space structures with the same characteristics as that of linear Landau damping of Alfvén waves in a 3D linear simulation. The continual occurrence of the velocity-space structures throughout the turbulence simulations suggests that the action of Landau damping may be responsible for the turbulent energy transfer to electrons in both 2D and 3D, and makes possible the subsequent irreversible heating of the plasma through collisional smoothing of the velocity-space fluctuations. Although, in the 2D case where variation along the equilibrium magnetic field is absent, it may be expected that Landau damping is not possible, a common trigonometric factor appears in the 2D resonant denominator, leaving the resonance condition unchanged from the 3D case. The evolution of the 2D and 3D cases is qualitatively similar. However, quantitatively the nonlinear energy cascade and subsequent dissipation is significantly slower in the 2D case.

Subject headings: plasma — turbulence — waves

1. Introduction

In a wide variety of space and astrophysical systems such as the solar corona, solar wind, the interstellar medium and galaxy clusters, plasma turbulence plays a governing role in the transfer of energy from large-scale motions down to small scales, where that energy is ultimately converted to plasma heat. A fundamental question at the frontier of astrophysics is what physical mechanisms determine the dissipation of the turbulence, specifically how the energy of the turbulent fluctuations in a weakly collisional plasma is ultimately converted to heat or other forms of particle energization.

To investigate numerically the dynamics of the collisionless wave-particle interactions that lead to damping of the turbulent electromagnetic fluctuations requires kinetic simulations, but their high-dimensionality requires significant computational power that often limits numerical studies to only two spatial dimensions (Gary et al. 2008; Parashar et al. 2009; Servidio et al. 2012; Verscharen et al. 2012; Wan et al. 2012; Markovskii & Vasquez 2013; Perrone et al. 2013; Wu et al. 2013b,a; Che et al. 2014; Haynes et al. 2014; Narita et al. 2014; Parashar et al. 2014; Franci et al. 2015). How this limitation to 2D constrains the available energy dissipation pathways remains an open question (Howes 2015; Wan et al. 2015; Servidio et al.

2015).

This work aims at providing a model of comparison between 2D and 3D turbulence systems in a low- β plasma, focusing on energy dissipation, and exploring the dynamics of distribution functions as a novel means to characterize the energy transfer mechanism in velocity space.

In the following, we present results from gyrokinetic simulations showing quantitative difference in the energy dissipation of 2D and 3D nonlinear turbulence simulations and the development of velocity-space structures that share the same characteristics as that of linear Landau damping of Alfvén waves in a 3D linear simulation. The velocity-space structures are observed throughout the entire evolution of both 2D and 3D turbulence simulations, implying the continual occurrence of Landau damping during the dissipation of turbulence in both systems. Although, in the 2D case with no variation along the equilibrium magnetic field, it may be expected that Landau damping is not possible, we explain why the limitation to 2D does not prohibit Landau damping. This 2D limitation does, however, alter the quantitative evolution of the energy, likely due to a less rapid nonlinear cascade of energy to small scales compared to the 3D case.

2. Simulation Code

The Astrophysical Gyrokinetics Code, or **AstroGK**, described in detail in Ref. (Numata et al. 2010), evolves the perturbed gyroaveraged distribution function $h_s(x, y, z, \lambda, \varepsilon)$ for each species s , the scalar potential φ , parallel vector potential A_{\parallel} , and the parallel magnetic field perturbation δB_{\parallel} according to the gyrokinetic equation and the gyroaveraged Maxwell's equations (Frieman & Chen 1982; Howes et al. 2006), where \parallel is along the total local magnetic field $\mathbf{B} = B_0 \hat{\mathbf{z}} + \delta \mathbf{B}$. The velocity-space coordinates are $\lambda = v_{\perp}^2/v^2$ and $\varepsilon = v^2/2$. The domain is a periodic box of size $L_{\perp}^2 \times L_z$, elongated along the equilibrium magnetic field, $\mathbf{B}_0 = B_0 \hat{\mathbf{z}}$. Note that, in the gyrokinetic formalism, all quantities may be rescaled to any parallel dimension satisfying $\epsilon \equiv L_{\perp}/L_z \ll 1$. Uniform Maxwellian equilibria for ions (protons) and electrons are used. Spatial dimensions (x, y) perpendicular to the equilibrium field are treated pseudospectrally; an upwind finite-difference scheme

is used in the parallel direction. Collisions are incorporated using a fully conservative, linearized Landau collision operator that includes energy diffusion and pitch-angle scattering due to electron-electron, ion-ion, and electron-ion collisions (Abel et al. 2008; Barnes et al. 2009), yielding an isotropic Maxwellian stationary solution.

3. Diagnostics

Two diagnostics are used to explore the energetics and velocity-space structure in the 2D and 3D turbulence simulations. The *energy diagnostic* examines the partitioning of energy among the terms of the fluctuating energy in the simulations. Consider a kinetic plasma with each species distribution function separated into an equilibrium and a fluctuating part, $f_s = F_{0s} + \delta f_s$. **AstroGK** evolves the perturbed distribution function, δf_s , making it possible to follow the exchange of energy within the *total fluctuating energy* (Howes et al. 2006; Brizard & Hahm 2007; Schekochihin et al. 2009) given by

$$\delta W = \int d^3 \mathbf{r} \left[\frac{|\delta \mathbf{B}|^2 + |\delta \mathbf{E}|^2}{8\pi} + \sum_s \left(\frac{1}{2} n_{0s} m_s |\delta \mathbf{u}_s|^2 + \frac{3}{2} \delta P_s \right) \right], \quad (1)$$

where s is the species index representing ions or electrons in each variable, n_{0s} the equilibrium density, m_s mass and $\delta \mathbf{u}_s$ the fluctuating bulk velocity; the *non-thermal energy* in the distribution function (minus bulk kinetic energy) is defined by $E_s^{(nt)} \equiv \int d^3 \mathbf{r} \frac{3}{2} \delta P_s \equiv \int d^3 \mathbf{r} \left(\int d^3 \mathbf{v} T_{0s} \delta f_s^2 / 2F_{0s} - \frac{1}{2} n_{0s} m_s |\delta \mathbf{u}_s|^2 \right)$ (TenBarge et al. 2014), where T_{0s} is the equilibrium temperature. The *turbulent energy* is defined as the sum of the electromagnetic field and the bulk kinetic energies (Howes 2015), $E^{(turb)} \equiv \int d^3 \mathbf{r} [(|\delta \mathbf{B}|^2 + |\delta \mathbf{E}|^2) / 8\pi + \sum_s \frac{1}{2} n_{0s} m_s |\delta \mathbf{u}_s|^2]$. This sum comprises the turbulent energy because the linear terms in the evolution equations (primarily the effect of magnetic tension) lead to an oscillatory sloshing of energy between magnetic and bulk kinetic energies. Note that δW includes neither the equilibrium thermal energy, $\frac{3}{2} n_{0s} T_{0s} = \int d^3 \mathbf{r} \int d^3 \mathbf{v} \frac{1}{2} m_s v^2 F_{0s}$, nor the equilibrium magnetic field energy, $\int d^3 \mathbf{r} B_0^2 / 8\pi$. Thus, the terms of δW represent the perturbed electromagnetic field energies, and the species bulk kinetic and non-thermal energies.

The flow of energy in our kinetic turbulence simulations follows a simple path. As the system evolves, first, nonlinear interactions transfer the turbulent energy from large to small spatial scales. When the energy has reached sufficiently small spatial scales, collisionless wave-particle interactions transfer energy from the electromagnetic fields to non-thermal energy in the particle distributions. This non-thermal energy in δf_s manifests as small-scale structures in the velocity space, which are ultimately smoothed out by collisions, irreversibly converting the non-thermal energy into thermal energy, and thereby increasing the entropy of the plasma (Howes et al. 2006). In *AstroGK*, the effect of collisions is to remove energy from δW . The collisional energy lost from δW , denoted $E_s^{(coll)}$, is tracked by the energy diagnostic, representing thermal heating of the species, but this energy is not fed back into the equilibrium thermal temperature, T_{0s} (Howes et al. 2006; Numata et al. 2010).

The *velocity-space diagnostic* probes structures in velocity space that arise from the collisionless damping of the turbulent fluctuations. To first-order in gyrokinetic theory (Howes et al. 2006), the distribution function is given by

$$f_s(v_{\parallel}, v_{\perp}) = \left(1 - \frac{q_s \varphi}{T_{0s}}\right) F_{0s}(v) + h_s(v_{\parallel}, v_{\perp}), \quad (2)$$

where $F_{0s} = (n_{0s}/\pi^{3/2}v_{ts}^3) \exp(-v^2/v_{ts}^2)$ is the equilibrium Maxwellian distribution, $q_s \varphi/T_{0s}$ is the Boltzmann term (q_s the species charge and φ the electric potential), h_s is the first-order gyroaveraged part of the perturbed distribution. The complementary distribution function (Schekochihin et al. 2009),

$$g_s(v_{\parallel}, v_{\perp}) = h_s(v_{\parallel}, v_{\perp}) - \frac{q_s F_{0s}}{T_{0s}} \left\langle \varphi - \frac{\mathbf{v}_{\perp} \cdot \mathbf{A}_{\perp}}{c} \right\rangle_{\mathbf{R}_s}, \quad (3)$$

where $\langle \dots \rangle$ represents gyroaveraging at constant guiding center \mathbf{R}_s , removes the effect of the perpendicular bulk flow of MHD Alfvén waves, allowing kinetic dynamics of collisionless damping to be more clearly seen.

4. Simulations

The 2D Orszag-Tang Vortex (OTV) problem (Orszag & Tang 1979), and various 3D general-

izations, have been widely used to study plasma turbulence (Politano et al. 1989; Dahlburg & Picone 1989; Picone & Dahlburg 1991; Politano et al. 1995; Grauer & Marliani 2000; Mininni et al. 2006; Parashar et al. 2009, 2014). We specify here a particular 3D formulation of the initial conditions (denoted *OTV3D*), given in Elsässer variables, $\mathbf{z}^{\pm} \equiv \delta \mathbf{u} \pm \delta \mathbf{B}/\sqrt{4\pi\rho_0}$, by

$$\begin{aligned} \frac{\mathbf{z}_1^+}{v_A} &= -\frac{2z_0}{v_A} \hat{\mathbf{x}} \sin(k_{\perp}y - k_{\parallel}z), \quad \frac{\mathbf{z}_1^-}{v_A} = 0 \\ \frac{\mathbf{z}_2^{\pm}}{v_A} &= \frac{z_0}{v_A} \hat{\mathbf{y}} \sin(k_{\perp}x \mp k_{\parallel}z) \\ \frac{\mathbf{z}_3^{\pm}}{v_A} &= \pm \frac{z_0}{v_A} \hat{\mathbf{y}} \sin(2k_{\perp}x \mp k_{\parallel}z) \end{aligned} \quad (4)$$

where $v_A = B_0/\sqrt{4\pi\rho_0}$ is the Alfvén speed, $\rho_0 = m_i n_0$ is the ion mass density, $\delta \mathbf{u}$ and $\delta \mathbf{B}$ are perturbations in the ion bulk velocity and the magnetic field, and $k_{\perp} = 2\pi/L_{\perp}$ and $k_{\parallel} = 2\pi/L_z$ are positive constants. This 3D generalization consists of counterpropagating Alfvén waves along $B_0 \hat{\mathbf{z}}$. On the mid-plane ($z = 0$), the 3D formulation reduces to the familiar 2D OTV setup (*OTV2D*), given by

$$\begin{aligned} \delta \mathbf{u} &= \delta u [-\sin(k_{\perp}y)\hat{\mathbf{x}} + \sin(k_{\perp}x)\hat{\mathbf{y}}] \\ \delta \mathbf{B} &= \delta B [-\sin(k_{\perp}y)\hat{\mathbf{x}} + \sin(2k_{\perp}x)\hat{\mathbf{y}}], \end{aligned} \quad (5)$$

where $z_0 = \delta u = \delta B/\sqrt{4\pi\rho_0}$.

To resolve the kinetic mechanisms mediating the transfer of turbulent energy to plasma energy, it is necessary to follow the turbulent cascade from the inertial range ($k_{\perp}\rho_i \ll 1$) to below the electron scales ($k_{\perp}\rho_e > 1$) (TenBarge & Howes 2013; TenBarge et al. 2013; TenBarge et al. 2014). Therefore, we specify a reduced mass ratio, $m_i/m_e = 25$, which, in a simulation domain of $L_{\perp} = 8\pi\rho_i$ and dimensions $(n_x, n_y, n_z, n_{\lambda}, n_{\varepsilon}, n_s) = (128, 128, 32, 64, 32, 2)$ in 3D (with $n_z = 2$ in 2D), enables us to resolve a dynamic range of $0.25 \leq k_{\perp}\rho_i \leq 10.5$, or $0.05 \leq k_{\perp}\rho_e \leq 2.1$.

Plasma parameters are ion plasma beta $\beta_i = 8\pi n_i T_{0i}/B_0^2 = 0.01$ and $T_{0i}/T_{0e} = 1$. Under $\beta_i \ll 1$ conditions, the ion dynamics are expected to contribute negligibly to the collisionless damping via the Landau resonance. Collision frequencies of $\nu_i = 10^{-5}\omega_{A0}$ and $\nu_e = 0.05\omega_{A0}$ (where $\omega_{A0} \equiv k_{\parallel}v_A$ is a characteristic Alfvén wave frequency in 3D) are sufficient to keep velocity space

well resolved (Howes et al. 2008; Howes et al. 2011) and enable irreversible heating of the plasma species (Howes et al. 2006). We choose an initial amplitude that yields a nonlinearity parameter $\chi = k_{\perp} z_0 / (k_{\parallel} v_A) = 1$, corresponding to *critical balance* (Goldreich & Sridhar 1995), or a state of strong turbulence; the same amplitude z_0 is used in the 2D run. Time is normalized by the domain turnaround time $\tau_0 = L_{\perp} / z_0$ and velocity by the species thermal speed $v_{ts} = \sqrt{2T_{0s} / m_s}$.

Note that, for the reduced mass ratio, the low beta conditions satisfy $\beta_i < m_e / m_i$, so the Alfvén wave transitions to an inertial Alfvén wave (Thompson & Lysak 1996) at small scales. In 3D, the initial counterpropagating Alfvén waves at the perpendicular domain scale L_{\perp} have a frequency of $\omega = 0.93\omega_{A0}$, and the frequency drops slowly as the perpendicular scale decreases. Simulations with $\beta_i = 0.1$, in which the Alfvén wave transitions instead to a kinetic Alfvén wave at small scales, show results similar to those presented here, so we believe the physical mechanism reported here is robust for low- β plasmas.

5. Results

5.1. Evolution of the OTV

The OTV setup consists of an initial flow and current pattern, which breaks up into turbulence before $t = \tau_0$. We plot in Figure 1 the spatial profile of J_{\parallel} (color) and A_{\parallel} (contours) from the OTV2D and the $z = 0$ plane of the OTV3D simulations. At $t = 0.5\tau_0$, the initial double vortices near the center have merged completely in both cases, and thin current sheets have developed. Note that $t = 0.5\tau_0$ is roughly half of the Alfvén wave period, so the J_{\parallel} pattern at $z = 0$ in 3D appears π *out of phase* (opposite colors) relative to the 2D case. At $t = \tau_0$, J_{\parallel} in 3D returns to a configuration similar to the 2D case: negative (blue) current in the center surrounded by positive (red) currents. The nonlinear cascade of energy to small scales is more rapid in the 3D case, showing more energy in small-scale magnetic structures in Figure 1; this is supported by comparing the magnetic energy spectra (not shown).

5.2. Evolution of Energy

Next we consider the flow of energy from turbulent fluctuations to plasma heat. It is worth-

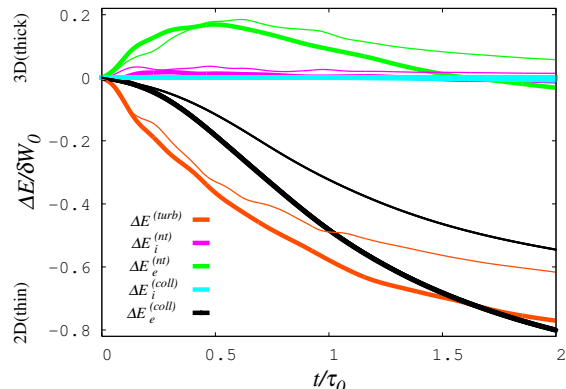


Fig. 2.— Change of energy over total initial fluctuating energy, $\Delta E / \delta W_0$, for the turbulent energy $E^{(turb)}$ (orange), the non-thermal energy $E_s^{(nt)}$ of ions (magenta) and electrons (green), the collisionally dissipated energy $E_s^{(coll)}$ for ions (cyan) and electrons (black). Line thickness indicates OTV3D (thick) or OTV2D (thin) simulations.

while mentioning the dominant components of the turbulent energy in our simulations. For low-frequency electromagnetic waves, $|\delta \mathbf{E}|^2 / |\delta \mathbf{B}|^2 \sim \mathcal{O}(v_A^2 / c^2)$, so the electric field energy is negligible in the non-relativistic limit (Howes et al. 2006, 2014). Throughout the evolution, the turbulent energy $E^{(turb)}$ is dominated by the perpendicular magnetic and perpendicular ion bulk kinetic energy (more than 75%). The parallel electron bulk kinetic energy, supporting the currents in the simulation, contributes less than 20% of the energy, but this is artificially large due to the small mass ratio chosen, $m_i / m_e = 25$; for a realistic mass ratio of 1836, it is not expected to contribute significantly to the energy budget. Finally, the parallel magnetic, parallel ion bulk kinetic, and perpendicular electron bulk kinetic energies contribute less than 7% of the turbulent energy.

Figure 2 shows the change in energy ΔE , relative to the initial total fluctuating energy δW_0 , for the turbulent $E^{(turb)}$ (orange), non-thermal $E_s^{(nt)}$ (magenta, green), and collisionally dissipated $E_s^{(coll)}$ (cyan, black) energies, where line thickness indicates OTV3D (thick) or OTV2D (thin) simulations. Initially, turbulent energy (orange) is dominantly transferred into electron non-thermal energy (green). Physically, this occurs

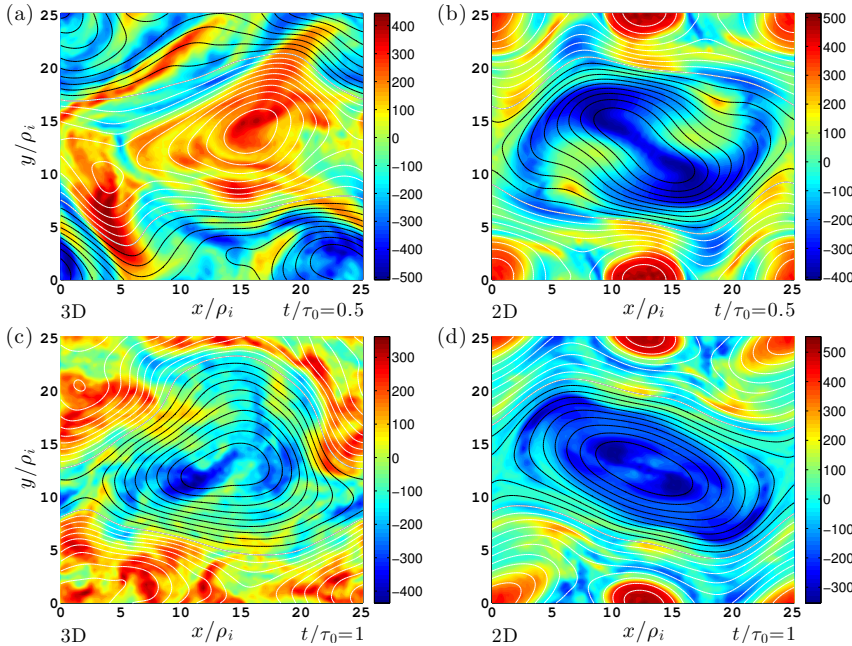


Fig. 1.— Spatial profile of J_{\parallel} (color) and A_{\parallel} (contours) on the $z = 0$ plane of the OTV3D (left) and OTV2D (right) simulations at $t/\tau_0 = 0.5$ (top) and $t/\tau_0 = 1$ (bottom). Contours represent positive (white) and negative (black) values of A_{\parallel} .

through a two-step process: (1) the turbulent energy is transferred nonlinearly to small spatial scales; and (2) at these small scales, collisionless wave-particle interactions transfer energy from the electromagnetic fields to the electrons as non-thermal energy in the velocity distribution, $E_e^{(nt)}$. At $t > 0.25\tau_0$, the electron non-thermal energy begins to be significantly collisionally dissipated (black), indicating the ultimate thermalization of electron energy (which `AstroGK` removes from δW). As expected, ions play a negligible role in the dissipation of the turbulent energy at $\beta_i \ll 1$.

The qualitative evolution of the 2D case is remarkably similar to the 3D case, suggesting that the same kinetic physical mechanisms mediate the dissipation in both cases. Despite this qualitative similarity, quantitatively, the dissipation rate is significantly faster in 3D. By $t = 2\tau_0$, the 3D simulation has dissipated 80% of δW_0 , indicating a strong turbulent cascade, but the 2D simulation has dissipated only 55%.

5.3. Landau damping

Landau damping (Landau 1946) is the mechanism by which particles absorb energy from parallel electric fields of waves in collisionless plasmas. Waves and particles interact strongly near the resonant velocity v_r when the Landau resonance condition, $\omega - k_{\parallel}v_{\parallel} = 0$, is satisfied, leading to an enhanced amplitude in the distribution function near v_r . The parallel electric field responsible for the interaction naturally generates velocity-space structure varying in v_{\parallel} . Furthermore, for Alfvén waves at $k_{\perp}\rho_e < 1$, linear gyrokinetic theory predicts that fluctuations in $g_e(v_{\parallel}, v_{\perp})/F_{0e}(v)$ via Landau damping vary only in v_{\parallel} , with little variation in v_{\perp} (Howes et al. 2006). Both an enhanced amplitude near the resonance condition and only v_{\parallel} variation are the two key characteristics of Landau damping to be focused on below.

5.4. Velocity-space structures indicating Landau damping

The velocity-space structures observed in both the 2D and 3D cases agree with the characteristics

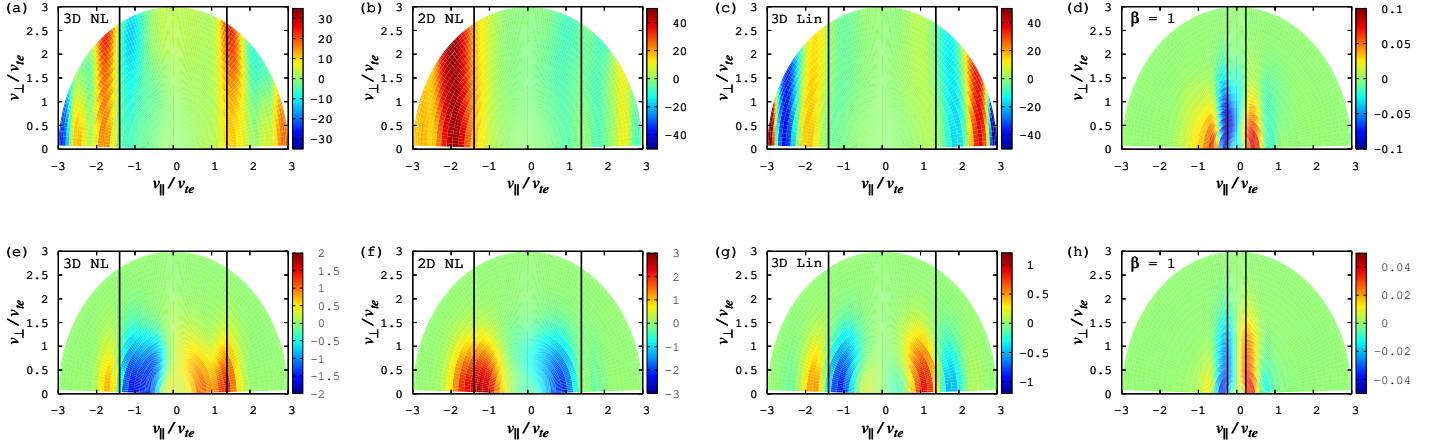


Fig. 3.— Velocity-space structures in a $\beta_i = 0.01$ plasma shown by plotting $g_e(v_{\parallel}, v_{\perp})/\epsilon F_{0e}(v)$ for (a) OTV3D, (b) OTV2D and (c) 3D linear simulations for the (1, 1) Fourier mode in the $z = 0$ plane, revealing only v_{\parallel} variation. Resonant signature as an enhancement of amplitude around the resonant velocities (vertical black lines) is shown by plotting $g_e(v_{\parallel}, v_{\perp})$ for (e) OTV3D, (f) OTV2D and (g) 3D linear cases; it is further demonstrated in (d) OTV3D and (h) 3D linear simulations for a $\beta_i = 1$ plasma. Animations for OTV3D and linear simulations of both β_i values, similar to (a) and (e), (c) and (g), are available.

of Landau damping that are also exhibited in linear simulations in which Alfvén waves are known to be Landau damped.

In Figure 3, for the (a) OTV3D and (b) OTV2D cases, we plot $g_e(v_{\parallel}, v_{\perp})/\epsilon F_{0e}(v)$ (the amplitude of g_e relative to F_{0e} , normalized by the gyrokinetic epsilon) for the perpendicular Fourier mode in the $z = 0$ plane, $(k_x \rho_i, k_y \rho_i, z) = (1, 1, 0)$, at the peak of the electron collisional dissipation rate at $t/\tau_0 \simeq 0.7$. The resonant velocities for this Alfvén mode are $|v_r| = |\omega/k_{\parallel}| \simeq 1.4v_{te}$ (vertical black lines), where ω/k_{\parallel} is given by linear kinetic theory. Note that this mode receives energy strictly via the turbulent nonlinear interactions that transfer energy from the larger scale initial modes. Plotted in (c) is the velocity-space characteristic of Landau damping in the $z = 0$ plane from a linear 3D simulation of two counterpropagating Alfvén waves with $(k_x \rho_i, k_y \rho_i, k_z L_z) = (1, 1, \pm 1)$, in which the waves are verified to Landau damp at the rate predicted by linear kinetic theory. In all of these plots, since $F_{0e}(v)$ is small at large v , division by $F_{0e}(v)$ emphasizes structures at larger v , thus enabling small-amplitude fluctuations near the tail of the distribution to be more clearly seen. This is good for revealing the overall profile of the variation. In

the plots (a)-(c), OTV3D, OTV2D and 3D linear simulations share the same strictly v_{\parallel} structure, consistent with the characteristic of Landau damping. The variation in OTV2D develops shorter scales, closely resembling those in OTV3D, at a later time, consistent with the slower evolution of OTV2D (see Figure 1).

Another observed characteristic in the turbulence simulations is an enhanced amplitude around v_r . This can be examined by plotting just $g_e(v_{\parallel}, v_{\perp})$ (instead of the relative amplitude). In Figure 3, we plot $g_e(v_{\parallel}, v_{\perp})$ for (e) OTV3D, (f) OTV2D and (g) 3D linear simulations, showing an enhancement of fluctuations near v_r . The specific profile varies from case to case, but they all share the same characteristic of exhibiting an increase in amplitude around v_r .

To confirm the robustness of the resonance signature, identical OTV3D and 3D linear simulations but with $\beta_i = 1$, in which, the resonance will occur at a much lower $|v_r| \simeq 0.24v_{te}$, for the same (1,1) mode, were performed. An enhanced amplitude is observed at the predicted lower v_r in $g_e(v_{\parallel}, v_{\perp})$ from (d) OTV3D and (h) 3D linear simulations, confirming the presence of Landau resonance. Supplemental movies further illustrate

the persistent signature around v_r throughout the time evolution of OTV3D and 3D linear simulations.

The velocity-space structures in Figure 3 provide a novel means for the characterization of the physical mechanism responsible for the collisionless damping of fluctuations in kinetic plasma turbulence. We find that both 2D and 3D simulations of strong plasma turbulence develop velocity-space characteristics indicative of Landau damping, namely, only v_{\parallel} variation and an enhanced amplitude around the resonant condition. This development of velocity-space structures facilitates the subsequent collisional dissipation of the non-thermal energy. Furthermore, the velocity-space characteristics in the nonlinear simulations appears very similar to that of *linear* Landau damping, suggesting the kinetic dissipation is largely linear in nature, supporting a recent theoretical prediction (Howes 2015).

Let us mention two additional points. First, the entropy cascade (Schekochihin et al. 2009; Tatsuno et al. 2009) is not expected to play a significant role for electrons in the transfer of energy to small velocity-space scales when $k_{\perp}\rho_e < 1$, and indeed we find little of the v_{\perp} variation predicted for this process. Second, a current sheet develops during the merging of the initial double vortices, and multiple thin current sheets arise later in both the 2D and 3D simulations (Figure 1). Despite the development and dissipation of these coherent structures, the velocity-space structures appears to be consistent with Landau damping, supporting speculation that Landau damping dominates dissipation of current sheets in collisionless 3D kinetic Alfvén wave turbulence (TenBarge & Howes 2013), and consistent with the interpretation of solar wind observations (Sahraoui et al. 2009) and evidence of Landau damping in 2D simulations of magnetic reconnection (Numata & Loureiro 2015).

5.5. Landau Damping in 2D?

For a 2D simulation with no variation along the equilibrium magnetic field $\mathbf{B}_0 = B_0\hat{\mathbf{z}}$, one may naively expect that Landau damping is prohibited. However, when there is an in-plane component such that the total field is $\mathbf{B} = B_0\hat{\mathbf{z}} + \delta B_{\perp}\hat{\mathbf{x}}$, the resonant denominator responsible for Landau damping becomes $\omega - k_x v_{\parallel} \sin\theta$, where $\sin\theta = \delta B_{\perp}/|\mathbf{B}|$. The frequency of linear Alfvén waves

propagating on the 2D plane is also modified to become $\omega = k_x v_A \sin\theta$. The trigonometric correction factors out, leaving a 2D resonant condition $v_{\parallel} \sim v_A$ that is essentially unchanged from the 3D case. This explains how Landau damping can potentially play an important role in energy dissipation in both 2D and 3D kinetic turbulence simulations. In 2D hybrid simulations of Alfvénic turbulence, cyclotron resonance is also observed (Hellinger et al. 2015).

6. Conclusions

Results from 2D and 3D nonlinear gyrokinetic simulations of plasma turbulence at $\beta_i \ll 1$ are presented. Qualitatively similar evolution of the energy flow from turbulent fluctuations to electron heat is observed in both 2D and 3D cases. Quantitatively, the nonlinear energy transfer and subsequent dissipation is substantially slower in the 2D case. In addition, the development of electron velocity-space structures is examined to characterize the nature of the dissipation process. We found that throughout the time evolution of both the 2D and 3D nonlinear simulations, fluctuations enhanced near the resonant velocity with only v_{\parallel} structure, characteristics shared by the linear Landau damping of Alfvén waves, are generated. This suggests the continual occurrence of Landau damping throughout the dissipation process and also indicates that this kinetic damping mechanism is essentially linear in nature (Howes 2015). This is further supported by complementary 3D nonlinear and linear kinetic simulations using $\beta_i = 1$, which are consistent with the role of Landau damping in 3D Landau-fluid simulations of Alfvénic turbulence (Passot et al. 2014). Despite naive expectations that Landau damping is ineffective in 2D, the action of Landau damping in 2D simulations is explained theoretically by a common trigonometric correction factor appearing in both the resonant denominator and the linear wave frequency, resulting in an essentially unchanged resonance condition. These results provide new information on the dynamics of distribution functions during the dissipation process and are consistent with previous finding that Landau damping likely plays a dominant role in energy transfer in plasma turbulence, even when current sheets develop and dissipate, as observed in 3D simulations of kinetic Alfvén wave turbulence

(TenBarge & Howes 2013; TenBarge et al. 2013) and 2D simulations of strong-guide-field magnetic reconnection (Numata & Loureiro 2015). Future studies require investigation of the connection between the turbulent fields and plasma particles in velocity space to determine the energy transfer between the fields and particles.

Supported by NSF CAREER Award AGS-1054061, NASA grant NNX10AC91G, NSF grant AGS-1331355, and US DOE grant DEFG0293ER54197. This work used the Extreme Science and Engineering Discovery Environment (XSEDE), which is supported by NSF grant ACI-1053575.

REFERENCES

- Abel, I. G., Barnes, M., Cowley, S. C., Dorland, W., & Schekochihin, A. A. 2008, *Phys. Plasmas*, 15, 122509
- Barnes, M., Abel, I. G., Dorland, W., et al. 2009, *Phys. Plasmas*, 16, 072107
- Brizard, A. J., & Hahm, T. S. 2007, *Rev. Mod. Phys.*, 79, 421
- Che, H., Goldstein, M. L., & Viñas, A. F. 2014, *Phys. Rev. Lett.*, 112, 061101
- Dahlburg, R. B., & Picone, J. M. 1989, *Phys. Fluids B*, 1, 2153
- Franci, L., Verdini, A., Matteini, L., Landi, S., & Hellinger, P. 2015, *The Astrophysical Journal Letters*, 804, L39
- Frieman, E. A., & Chen, L. 1982, *Phys. Fluids*, 25, 502
- Gary, S. P., Saito, S., & Li, H. 2008, *Geophys. Res. Lett.*, 35, 2104
- Goldreich, P., & Sridhar, S. 1995, *Astrophys. J.*, 438, 763
- Grauer, R., & Marliani, C. 2000, *Phys. Rev. Lett.*, 84, 4850
- Haynes, C. T., Burgess, D., & Camporeale, E. 2014, *Astrophys. J.*, 783, 38
- Hellinger, P., Matteini, L., Landi, S., et al. 2015, *The Astrophysical Journal Letters*, 811, L32
- Howes, G. G. 2015, *Philosophical Transactions of the Royal Society of London A: Mathematical, Physical and Engineering Sciences*, 373, 20140145
- Howes, G. G. 2015, *Journal of Plasma Physics*, 81, 3203
- Howes, G. G., Cowley, S. C., Dorland, W., et al. 2006, *Astrophys. J.*, 651, 590
- Howes, G. G., Dorland, W., Cowley, S. C., et al. 2008, *Phys. Rev. Lett.*, 100, 065004
- Howes, G. G., Klein, K. G., & TenBarge, J. M. 2014, *Astrophys. J.*, 789, 106
- Howes, G. G., TenBarge, J. M., Dorland, W., et al. 2011, *Phys. Rev. Lett.*, 107, 035004
- Landau, L. D. 1946, *Zh. Eksp. Teor. Fiz.*, 16, 574
- Markovskii, S. A., & Vasquez, B. J. 2013, *Astrophys. J.*, 768, 62
- Mininni, P. D., Pouquet, A. G., & Montgomery, D. C. 2006, *Phys. Rev. Lett.*, 97, 244503
- Narita, Y., Comisel, H., & Motschmann, U. 2014, *Frontiers in Phys.*, 2, 13
- Numata, R., Howes, G. G., Tatsuno, T., Barnes, M., & Dorland, W. 2010, *J. Comp. Phys.*, 229, 9347
- Numata, R., & Loureiro, N. F. 2015, *Journal of Plasma Physics*, 81, 3001
- Orszag, S. A., & Tang, C.-M. 1979, *J. Fluid Mech.*, 90, 129
- Parashar, T. N., Shay, M. A., Cassak, P. A., & Matthaeus, W. H. 2009, *Phys. Plasmas*, 16, 032310
- Parashar, T. N., Vasquez, B. J., & Markovskii, S. A. 2014, *Physics of Plasmas*, 21, 022301
- Passot, T., Henri, P., Laveder, D., & Sulem, P.-L. 2014, *The European Physical Journal D*, 68, 1
- Perrone, D., Valentini, F., Servidio, S., Dalena, S., & Veltri, P. 2013, *Astrophys. J.*, 762, 99
- Picone, J. M., & Dahlburg, R. B. 1991, *Phys. Fluids B*, 3, 29

- Politano, H., Pouquet, A., & Sulem, P. L. 1989, Phys. Fluids B, 1, 2330
- . 1995, Physics of Plasmas, 2, 2931
- Sahraoui, F., Goldstein, M. L., Robert, P., & Khotyaintsev, Y. V. 2009, Phys. Rev. Lett., 102, 231102
- Schekochihin, A. A., Cowley, S. C., Dorland, W., et al. 2009, Astrophys. J. Supp., 182, 310
- Servidio, S., Valentini, F., Califano, F., & Veltri, P. 2012, Phys. Rev. Lett., 108, 045001
- Servidio, S., Valentini, F., Perrone, D., et al. 2015, Journal of Plasma Physics, 81, 1
- Tatsuno, T., Schekochihin, A. A., Dorland, W., et al. 2009, Phys. Rev. Lett., 103, 015003
- TenBarge, J. M., Daughton, W., Karimabadi, H., Howes, G. G., & Dorland, W. 2014, Phys. Plasmas, 21, 020708
- TenBarge, J. M., & Howes, G. G. 2013, Astrophys. J. Lett., 771, L27
- TenBarge, J. M., Howes, G. G., & Dorland, W. 2013, Astrophys. J., 774, 139
- Thompson, B. J., & Lysak, R. L. 1996, J. Geophys. Res., 101, 5359
- Verscharen, D., Marsch, E., Motschmann, U., & Müller, J. 2012, Phys. Plasmas, 19, 022305
- Wan, M., Matthaeus, W. H., Roytershteyn, V., et al. 2015, Phys. Rev. Lett., 114, 175002
- Wan, M., Matthaeus, W. H., Karimabadi, H., et al. 2012, Phys. Rev. Lett., 109, 195001
- Wu, P., Wan, M., Matthaeus, W. H., Shay, M. A., & Swisdak, M. 2013a, Phys. Rev. Lett., 111, 121105
- Wu, P., Perri, S., Osman, K., et al. 2013b, Astrophys. J. Lett., 763, L30